Journal of Chromatography A, 1236 (2012) 77–89

Contents lists available at SciVerse ScienceDirect

Journal of Chromatography A

journal homepage: www.elsevier.com/locate/chroma

Quantifying injection solvent effects in reversed-phase liquid chromatography

Bradley J. VanMiddlesworth, John G. Dorsey*

Department of Chemistry and Biochemistry, Florida State University, Tallahassee, FL 32306-4390, USA

ARTICLE INFO

Article history:
Received 5 October 2011
Received in revised form 27 February 2012
Accepted 28 February 2012
Available online 7 March 2012

Keywords:
Hydrophobic subtraction model
Injection solvent
Diluent
Excess adsorption isotherm

ABSTRACT

Peak distortion due to the injection was measured as a function of injection solvent strength, volume, mass, retention factor, and column selectivity. The concept of a method's sensitivity (s) to injection solvent strength was mathematically defined as a vector of theoretical plate counts compared to an ideal vector that does not change with injection solvent strength. Near ideal sensitivity ($s > 0.90$) was measured on all columns with all analytes in low volume injections of 1.25 μL. Increasing the injection volume reduces the measured sensitivity from ideality to a greater extent than increasing the injection mass, with differing values for each column. Using column parameters measured from the hydrophobic-subtraction model and fitting parameters from the acetonitrile excess adsorption isotherm, differences among the columns studied are explained. Decreased ligand density and increased silanol activity provide a consistent peak shape with changes in injection volume or solvent strength. For method development, a quick test is suggested with the ratio of hydrophobic-subtraction column parameters, H/A, to predict the injection solvent sensitivity of a column. As H/A decreases, the sensitivity to injection solvent worsens. Sensitivity to organic modifiers other than acetonitrile are predicted with cited sorbed layer thickness, such that MeOH > EtOH > IPA ≈ THF ≈ MeCN, i.e., a strong MeOH diluent is more ideal (better) than a strong MeCN diluent.

1. Introduction

All samples must be dissolved in a diluent prior to injecting onto a liquid chromatographic column. For most methods, the diluent of choice is the mobile phase, and has been noted to give the best results [1]. Injection of any other solvent can be modeled as a step gradient with strength relative to the mobile phase. Increased strength of the injection solvent has been reported to cause distorted band shapes, shoulders on main peaks, peak splitting and peak tailing, particularly for early eluting peaks. Conversely, a decreased strength of the injection solvent is described to focus analytes at the head of the column [1–6]. Negative effects can be mitigated by reducing the sample mass or sample volume injected. However, there are cases when methods must use a high mass or volume load, such as in impurity profile analysis where the main peak is of significantly higher concentration than trace impurities. Additionally, in two-dimensional chromatography it is advantageous to have a large modulation volume between the dimensions to increase the available time of analysis to the second dimension. This becomes a significant problem when the modes of operation have sufficiently different mobile phases [7], or when a gradient is applied in the first dimension.

Strong injection solvents are more common in RPLC as they tend to solubilize analytes readily. Expectedly, with a strong injection solvent, analytes will be retained less for the duration spent within the injection plug. Loeser et al. [8,9] reported that peak distortion occurs for analytes that elute after the injection plug in highly aqueous mobile phases. When the injection solvent is strongly retained at the head of the column, less retained analytes migrate past the solvent plug and are retained by an axially homogeneous mobile phase-stationary phase system. Analytes that are more retained than the injection plug will spend a larger amount of time within the plug. If the analyte has different thermodynamics of retention in the injection plug when compared to the mobile phase-stationary phase system, then peak distortion will result in a case similar to the resistance to mass transfer from the stationary phase. With sufficiently different retention, the multiple of zones from the injection solvent-mobile phase mismatch will cause a peak to shoulder or split. Three zones can be imagined – (1) Concentration band of an analyte that migrates faster than the injection solvent, partitioning between mobile phase and stationary phase. (2) Concentration band of an analyte that migrates with the injection solvent, partitioning between the injection solvent band and the stationary phase. (3) Concentration band of an analyte that migrates slower than the injection solvent, partitioning between the mobile phase and the stationary phase. These concentration bands can overlap to produce a shoulder or separate from one another to produce a split peak.

* Corresponding author. Tel.: +1 850 644 4496.
E-mail address: dorsey@chem.fsu.edu (J.G. Dorsey).

0021-9673/$ – see front matter © 2012 Elsevier B.V. All rights reserved.
doi:10.1016/j.chroma.2012.02.075

Since injection solvent effects are fundamentally a retention effect, all variables effecting retention can arguably affect the sensitivity an analyte-column pair has to the injection solvent. Current understanding of a hydrophobic retention mechanism considers a three phase system: (1) mobile phase, (2) sorbed organic layer and (3) stationary phase ligands. Kazakevich et al. [10] derived an equation to model the change in retention volume (V_R) as a function of mobile phase composition (C_{el}):

$$V_R(C_{el}) = V_0 - V_S + K_P(C_{el})[V_S + SK_H] \quad (1a)$$

where V_0 is the volume of liquid phase in the column (mL), V_S is the volume of the adsorbed layer of organic modifier (mL), $K_P(C_{el})$ is the distribution coefficient of the analyte between the mobile phase and the adsorbed phase, S is the surface area of the adsorbent (m^2), and K_H is the Henry constant for the analyte adsorption from the pure organic adsorbed layer onto the surface of the bonded phase. K_H can be calculated from the retention volume of the analyte using neat organic modifier:

$$K_H = \frac{V_R(100) - V_0}{S} \quad (1b)$$

$K_P(C_{el})$ can be calculated by the distribution of the analyte in a vapor–liquid system using headspace GC, where the liquid system is either the neat organic liquid (C_{100}) or a mixture of water:organic (C_{el}). Then $K_P(C_{el})$ is $K_{(org\text{-}vap)}/K_{(el\text{-}vap)}$. Alkylbenzene homologues and 2-butanone were modeled and fit well to the chromatographic measurements.

For charged analytes, retention is also a function of the ionization state, which is a function of the pK_a of the analyte and the pH of the solvent [11]. To date, there has been no systematic investigation to the injection solvent sensitivity of ionizable analytes in comparison to non-polar compounds. Modeling the retention of ionizable analytes as a function of pH, organic modifier, and temperature is a far more difficult calculation, but has been recently described [12].

As shown by Hoffman et al. [3,4] using both simulation and experimental results, with slight changes in retention, the concentration profile of an analyte will tend to widen and become asymmetric. This suggests that efficiency calculations are a useful measure of injection solvent effects on the band profile of analytes. The Foley–Dorsey equation [13] for efficiency (N) quantitatively accounts for both a change in peak width and asymmetry:

$$N = \frac{41.7(t_R/W_{10\%})^2}{1.25 + As_{10\%}} \quad (2)$$

where t_R is the retention time at peak maximum, and $W_{10\%}$ and $As_{10\%}$ are the width and asymmetry of the peak at 10% height, respectively. $As_{10\%}$ is defined as the ratio of the half-widths of the peak A and B, measured from the leading edge of the peak to a normal drawn from peak apex to baseline, then from the normal to the trailing edge, respectively. $As_{10\%}$ is greater than unity in the calculation of theoretical plates, using either B/A for tailing peaks or A/B for fronting peaks. In general, chromatographic peaks tail, but in the case of injection solvent effect it is more common for peaks to front.

Other work has highlighted viscosity mismatch of the mobile phase and injection solvent as the source for injection solvent effects on peak shape. Castells et al. [14,15] first described this problem as the onset of viscous fingering. It was concluded that viscous fingering was a function of the magnitude of the viscosity mismatch, flow rate, sample volume and mass, and retention factor. Catchpoole et al. [16] first visualized the viscous fingering phenomenon in a 17 mm i.d. chromatographic column for an unretained marker. Though the degree of fingering was significant within the column at mismatch magnitudes of 0.17 cP, the band profiles detected post-column were only slightly distorted. At 0.49 cP the band profile was significantly distorted when compared to an injection without viscous fingering. Shalliker and Guiochon [17] extended the study with retained solutes in a 4.6 mm i.d. analytical sized column. Viscosity contrasts up to 1.283 cP did not elicit peak shouldering, though there was significant increase in the peak variance as a function of injection solvent and viscosity mismatch magnitude for analytes with retention factors of <5. It was suggested that this effect would be measurable for compounds that were more retained.

It is particularly difficult to segregate the effects of solvent strength and viscosity mismatches as changing the organic modifier content of the injection solvent affects both variables simultaneously. We do not distinguish these effects here and will focus only on the content of the injection solvent as a function of solvent strength. The largest magnitude of solvent mismatch in this work is 0.54 cP for the Section 4.1 and 0.63 cP for Section 4.4 [18]. Though it cannot be determined, we will assume that these are within the pre-viscous fingering region.

The aim of this work is to develop and apply a method on multiple columns to quantify the sensitivity to injection solvent strength for non-polar and basic analytes, with specific regard to water–acetonitrile mixtures as a solvent. Using the Foley–Dorsey equation for theoretical plate count as a desirability function, we investigate the effects of injection solvent on retention time (t_R), peak width at 10% peak height ($W_{10\%}$), and asymmetry at 10% peak height ($As_{10\%}$). We show a correlation to the hydrophobic-subtraction model coefficients and acetonitrile adsorption isotherms to aid in column-injection solvent pair selection.

2. Theory

2.1. Hydrophobic-subtraction (H-S) model

Reversed-phase column selectivity can be modeled by:

$$\log \alpha \equiv \log\left(\frac{k'}{k'_{ref}}\right) = \eta' H - \sigma' S^* + \beta' A + \alpha' B + \kappa' C \quad (3)$$

where the separation factor, α, is the logarithm of the ratio of the retention factors of test analytes, k', to a reference analyte, k'_{ref}, which is generally ethyl benzene [19]. The solute parameters describe the relative properties that contribute to retention in reversed-phase chromatography, namely hydrophobicity (η'), molecular "bulkiness" (σ'), hydrogen-bond basicity (β'), hydrogen-bond acidity (α'), and approximate charge (κ'). These solute parameters are a function of the separation conditions and have been calculated for the set of test analytes in a mobile phase of 50% 60 mM phosphate buffer (pH 2.8):50% MeCN (v/v) at 35 °C for alkyl and polar-embedded stationary phases as reported in Refs. [20,21], respectively. The parameters (H, S^*, A, B, C) are the complementary interactions of the column and describe the hydrophobicity, steric hindrance, hydrogen-bond acidity, hydrogen-bond basicity, and cation exchange activity at a given pH, respectively. Average C18 columns of type-B silica will have H equal to unity, and remaining parameters equal to zero. These values should be separation-condition independent, with exception to the cation-exchange activity being dependent on the pH of the mobile phase [22]. Column parameters for a large set of columns are accessible in the USP-PQRI database (http://www.usp.org/USPNF/columnsDB.html).

The physical and chemical origins of these column parameters have been described in detail in Ref. [23]. Parameters H and S are functions of stationary phase ligand length (C8 vs. C18), bonding density, side group (dimethyl vs. diisopropyl), and pore diameter. Parameters A and C are a function of the number of protonated (i.e., neutral) and ionized silanols, respectively. Parameter B is

considered to be a function of sorbed water in the phase, and is significantly higher for polar-embedded and polar-endcapped phases than alkyl phases.

2.2. Acetonitrile excess adsorption isotherm

The excess adsorption isotherm of organic modifiers can be measured by the minor disturbance method where a plug of organic-modifier-rich injection solvent is made onto a column that has been equilibrated with a mobile phase of organic modifier concentration, C_{el} [24,25]. From the retention volume of a minor disturbance $V_R(C_{el})$ in the baseline and the thermodynamic void volume V_m, the excess organic amount $n^e_{org}(C_{el})$ (mols) can be written as:

$$n^e_{org}(C_{el}) = \int_0^C (V_R - V_M)\delta C_{el} \tag{4a}$$

where V_M can be calculated by integration the retention times, V_R:

$$V_M = \frac{1}{C_{max}} \int_0^{C_{el}=C_{max}} V_R(C_{el})\delta C_{el} \tag{4b}$$

Alternatively, if the step values for δC_{el} are constant, then V_M is the mean of V_R. From n^e_{org}, the fraction absorbed at each mobile phase concentration x^a_{org} can be calculated by:

$$x^a_{org} = \frac{Stx^l + a^*_{aq} n^e_{org}}{St + (a^*_{aq} - a^*_{org})n^e_{org}} \tag{5}$$

where S is the absorbent surface area (m^2), t is the number of sorbed monolayers of organic modifier, x^l is the molar fraction of organic in the mobile phase, and a^* is the molar surface area of the pure components of the mobile phase as noted organic (org) or aqueous (aq). At 25 °C, a^* is 0.0776 m^2/μmol and 0.159 m^2/μmol for water and acetonitrile, respectively, estimated by comparison to the space requirement of nitrogen [26].

The number of monolayers of organic modifier is chosen by a convention where the value gives $\delta x^a_{org}/\delta x^l_{org} = 0$ at the inflection point, $x^l_{org} = I$, of the negative portion of $\delta n^e_{org}/\delta x^l_{org}$, given by:

$$t = \frac{-1}{S}\left(\left[\frac{\delta n^e_{org}}{\delta x^l_{org}}\right]_I ([x^l_{org}]_I a^*_{org} + \{1 - [x^l_{org}]_I\}a^*_{aq}) + (a^*_{aq} - a^*_{org})[n^e_{org}]_I\right) \tag{6}$$

Both t and I are found simultaneously by fitting $\delta x^a_{org}/\delta x^l_{org}$ with an arbitrarily high order polynomial, adjusting I, and solving $\delta x^a_{org}/\delta x^l_{org} = 0$ while constraining $\lim_{x\to I-} \delta x^a_{org}/\delta x^l_{org} < 0$ and $\lim_{x\to I+} \delta x^a_{org}/\delta x^l_{org} < 0$. For reversed phase modified silica with acetonitrile as a modifier, $t \approx 3$ and is a function of ligand length [10], ligand density [27], temperature, and pressure [28]. Knowing t, a function can be fit to the data of $n^e_{org}(x^l_{org})$:

$$n^e_{org}(x^l_{org}) = St\left(\varepsilon\frac{(K_{C18} - 1)x^e_{org}(1 - x^e_{org})}{K_{C18}a^*_{org}x^l_{org} + a^*_{aq}(1 - x^l_{org})} + [1 - \varepsilon]\frac{(K_{OH} - 1)x^e_{org}(1 - x^e_{org})}{K_{OH}a^*_{org}x^l_{org} + a^*_{aq}(1 - x^l_{org})}\right) \tag{7}$$

where ε is the surface heterogeneity and is roughly the fraction of surface area covered by the modifier ligand, and K_{C18} and K_{OH} are the equilibrium constants of the adsorption of the organic modifier to the ligand and silanols, respectively, for a special case in which the molecular sizes of the modifier and water are considered equivalent. These parameters are found simultaneously by maximizing r^2 of the fit in a regression.

Extensive discussion regarding the minor disturbance method and the underlying theory can be found in Ref. [26].

3. Experimental

3.1. Reagents

All water used was purified to a resistance of approximately 18 MΩ-cm using a Barnstead (Dubuque, IA, USA) NANOPure Diamond water purification system. HPLC grade acetonitrile (MeCN) was obtained from Sigma–Aldrich (St. Louis, MO, USA). Methyl ketones C3–C7 (acetone, butanone, 2-pentanone, 2-hexanone, and 2-heptanone) and lidocaine were obtained from Fisher Chemicals (Fair Lawn, NJ). Non-buffered mobile phase for the methyl ketone study was prepared by mixing the appropriate volumes of MeCN and H_2O then vacuum filtered through 0.45 μm nylon filter prior to use. Buffered mobile phase for the lidocaine study was prepared by mixing citric acid and sodium citrate monobasic in proportion to give 13.5 mM citrate concentration and a pH of ~2.8 prior to mixing with MeCN. Injection solvents were prepared by first adding analytes to the appropriate amount of MeCN, then diluted with water. All hydro-organic fractions are reported as volume-to-volume percents. All figures of merit (retention time, width, asymmetry, and plate count) reported were the average of three repetitive injections.

3.2. Liquid chromatography instrumentation

A Shimadzu LC-10 stack (Kyoto, Japan) was used for this study, including LC-10ADVP gradient pump outfitted with a DGU-14A inline degasser and an FCV-10ALVP quaternary proportioning valve, an SIL-10A auto injector with a 50 μL injection loop, an SPD-10A UV-vis detector set to 254 nm and 10 Hz data rate, and an SCL-10AVP system controller. All data were collected and analyzed using Class-VP version 5.032 software. Four stationary phases from Agilent Technologies were evaluated: Poroshell EC-C18, Zorbax 300Extend-C18, Zorbax SB-C18, and Zorbax Bonus-RP. The first column listed is packed with superficially porous silica, the remaining are fully porous silica. The last column listed has a polar embedded amide linker. Column parameters are listed in Table 1 [29]. Columns were chosen specifically for the ligand chemistry and bonding density. Temperature was kept constant via column jacket and circulator, though mobile phase was not preheated due to the ΔT from ambient being ≤5 °C for the injection solvent study and adsorption isotherms.

3.3. Liquid chromatography methods

3.3.1. Injection solvent – methyl ketones

Samples of three concentrations, 1.0 mg/mL, 2.0 mg/mL, and 4.0 mg/mL were diluted in regularly varied solvent strengths of water:acetonitrile mixtures from 10% MeCN to 100% MeCN in steps of 10%, for a total of 30 samples. Injection volumes varied for each concentration to compare equal and changing sample masses. Combinations were (1) 30 μL of 1.0 mg/mL, (2) 15 μL of 1 mg/mL, (3) 15 μL of 2 mg/mL, (4) 15 μL of 4 mg/mL, (5) 7.5 μL of 4 mg/mL, and (6) 1.25 μL of 4 mg/mL for a total of 180 injections per column. Fig. 1 shows a typical series of chromatograms as the injection solvent is strengthened from 10% to 100% MeCN. Near ideal sensitivity ($0.97 \le s \le 0.99$) is obtained from the small mass-small volume injections, 6. The remaining results are compared by static mass and changing volume (1, 3, 5) or by static volume and changing mass (2, 3, 4). The mobile phase was a premixed 60% H_2O:40% MeCN. Volume flow rate was set to 1.00 mL/min. Temperature was kept constant at 25 °C.

Table 1
Parameters of columns used in this work, as reported by manufacturer. Bonding density calculated by Ref. [24].

Column	Poroshell 120 EC-C18	Zorbax SB-C18	Zorbax 300Extend-C18	Zorbax Bonus-RP
d_p	2.7 μm	5 μm	3.5 μm	3.5 μm
Pore diameter	120 Å	80 Å	300 Å	80 Å
Surface area	120 m^2/g	180 m^2/g	45 m^2/g	180 m^2/g
Carbon load	8%	10%	4%	9.5%
Bonding density (μmol/m^2)	3.02	2.04	3.81	2.41
Dimensions	4.6 mm × 100 mm	4.6 mm × 150 mm	4.6 mm × 100 mm	4.6 mm × 75 mm
Ligand	Propylene-bridged methyl octadecylsilane	Diisobutyl octadecylsilane	Propylene-bridged methyl octadecylsilane	Diisopropyl butadecylsilane
Encapped?	Double	N	Double	Triple
Polar embedded?	N	N	N	Amide linker

For each injection, the peak variance due to the injection volume was calculated by [30]:

$$W^2_{10\%,\mathrm{inj}} = \frac{18.42V^2_{\mathrm{inj}}}{12} \quad (8)$$

where $W_{10\%,\mathrm{inj}}$ is the width of the peak due to the injection volume and V_{inj} is the injection volume. 18.42 is a conversion factor from variance to peak width at 10% height per the Gaussian formula [13]. This width was subtracted from the measured width $W_{10\%,\mathrm{total}}$ to calculate the width increase caused by the injection solvent strength $W_{10\%,\mathrm{col}}$:

$$W^2_{10\%,\mathrm{total}} - W^2_{10\%,\mathrm{inj}} = W^2_{10\%,\mathrm{col}} \quad (9)$$

3.3.2. Injection solvent – lidocaine

Similar to the methyl ketone study, three concentrations were used: 0.1 mg/mL, 0.2 mg/mL, and 0.4 mg/mL. All other conditions were kept the same, i.e., injection volume and injection solvent choice. This ensured that no sample overloading occurred on any of the four columns studied. The mobile phase was a premixed 75% 13.5 mM citrate buffer (pH ∼ 2.8):25% MeCN. Volume flow rate was set to 1.00 mL/min. Temperature was kept constant at 25 °C.

3.3.3. Hydrophobic-subtraction model

Conditions were as described in [31] for all columns studied. The solute parameters from Ref. [20] were used for 17 analytes on the alkyl phases (Poroshell EC-C18, Extend300-C18, and Stablebond-C18): thiourea, ethylbenzene, acetophenone, benzonitrile, anisole,

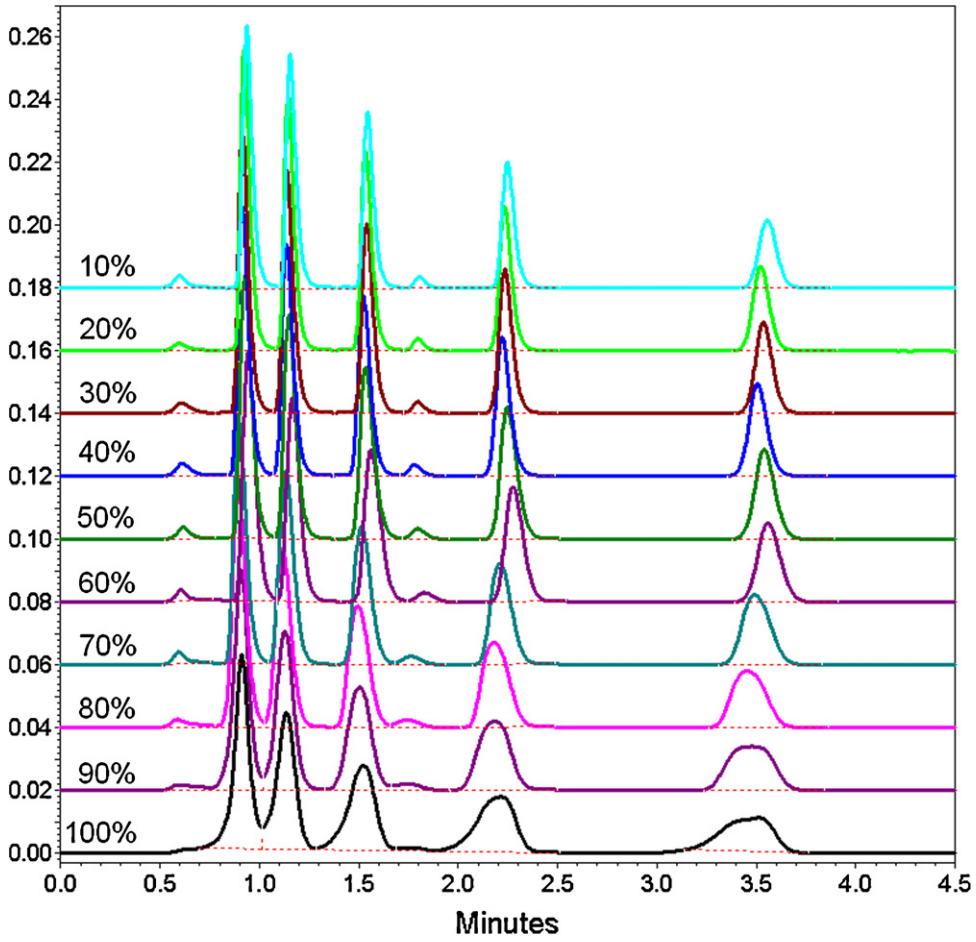

Fig. 1. Chromatograms showing the effects of injection solvent on peak shape of homologous series of methyl ketones, C3–C7. From top to bottom the injection solvent strength is varied from 10% to 100% MeCN, in steps of 10% increments. Column, injection volume, injection mass, mobile phase: Zorbax Bonus-RP, 30 μL, 30 μg, 40% MeCN in water.

toluene, 4-nitrophenol, 5-phenylpentanol, 5,5-diphenylhydantoin, cis-chalcone, trans-chalcone, N,N-dimethylacetamide, N,N-diethylacetamide, 4-n-butylbenzoic acid, mefenamic acid, nortriptyline, and amitriptyline. For the polar-embedded column (Bonus-RP), the solute parameters from Ref. [21] were used with addition of cis-4-nitro-chalcone, trans-4-nitro-chalcone, and *p*-chlorophenol. 5,5-diphenylhydantoin was not used to calculate the column parameters of the Bonus-RP phase. Amitriptyline and thiourea were injected as single components on the Bonus-RP due to co-elution.

Premixed 50% 60 mM Phosphate buffer (pH = 2.8):50% MeCN mobile phase was used as the injection solvent, with exception of the chalcones and mefenamic acid, which were first dissolved in 100% MeCN then added to the separation mixtures. The chalcones were irradiated with UV for at least 30 min prior to injection. Injection amount for each analyte was 500 ng, with exception of 4-nitro-chalcone, which was only slightly soluble in MeCN. Each retention time was an average of triplicate injections detected at 215 nm. Temperature was kept constant at 35 °C via column jacket.

3.3.4. Acetonitrile excess adsorption isotherm

For the minor disturbance method, each column was equilibrated in regularly stepped mobile phase (10%, 20%, 30%. MeCN) for at least 30 mL at 1.00 mL/min. Mobile phases were dynamically mixed via low-pressure quaternary proportioning valve with 100% H_2O in reservoir A and 100% MeCN in reservoir B. Mean retention times of triplicate injections of 10 μL and 1 μL of 100%MeCN were measured for V_R in Eqs. (4a) and (4b). Detector wavelength was set to 195 nm. Because of the very low analyte signal, and relatively high background signal, the waveform of the gradient mixer was evident in the chromatograms, and affected the precision of the retention time. For all columns at all mobile phase concentrations, the maximum and minimum %RSD of any triplicate injection was 2.3% and 0.2%. Temperature was kept constant at 25 °C via column jacket.

4. Results and discussion

4.1. Injection solvent sensitivity, s, of methyl ketones

Methyl ketones are ideal analytes for studying injection solvent effects due to the solubility in a range of aqueous MeCN mixtures. Figs. 2–5 show the effect of sample injection solvent strength on chromatographic figures of merit from Eq. (2) for three different injection volumes or injection masses. It can be seen from Fig. 2 that changing the injection solvent strength does not significantly change the retention time of the methyl ketones in any volume or mass measured on the Poroshell column, and holds true for the three other columns. There is a slight decrease in the values, on the Poroshell column from 10% to 100% MeCN, but the effect on efficiency is minor. On the Poroshell column, there is a 3.5% efficiency decrease of 2-heptanone due solely to the retention time shift from the maximum efficiency at the 1.25 μL, 5 μg, 100% MeCN injection (low volume, low mass) to the minimum efficiency of the 30 μL, 30 μg, 100% MeCN. This is expected, as the thermodynamics of retention for the peak maxima are affected by the injection solvent for only a small fraction of the total time on column [4]. It is unknown if the systematic differences in retention for some injections, e.g., 20% MeCN in Fig. 2, are an artifact of the instrumentation or are caused by true physico-chemical phenomena. We suspect the former as there is no correlation of systematic differences between columns, i.e., 20% MeCN does not give systematically increased retention times on the Zorbax 300Extend-C18 column, though for the purpose of this manuscript the trends within and between the columns are discussed.

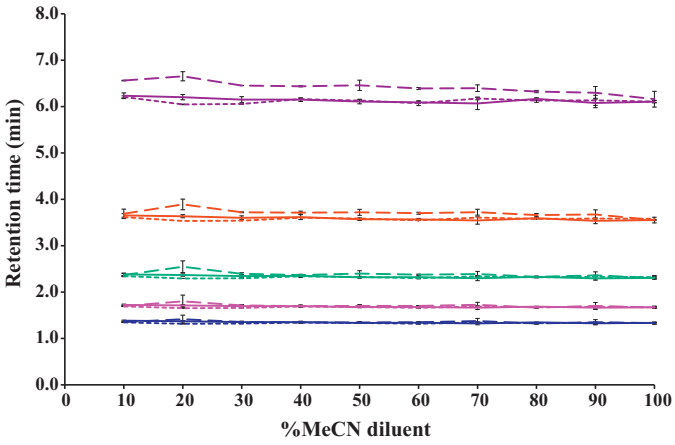

Fig. 2. Change in retention time with injection solvent strength. Analytes: acetone – dark blue, 2-butanone – pink, 2-pentanone – green, 2-hexanone – red, 2-heptanone – violet. Injection volumes: solid line – 30 μL, dashed line – 15 μL, dotted line – 7.5 μL. Injection mass: 30 μg. Column: Poroshell 120 EC-C18. (For interpretation of the references to color in this figure legend, the reader is referred to the web version of the article.)

The change in width at 10% height as a function of injection solvent is shown in Fig. 3A with injection volume and B with injection mass. In all four columns studied, injection mass has no significant effect on the width of the resulting peak, and reducing the

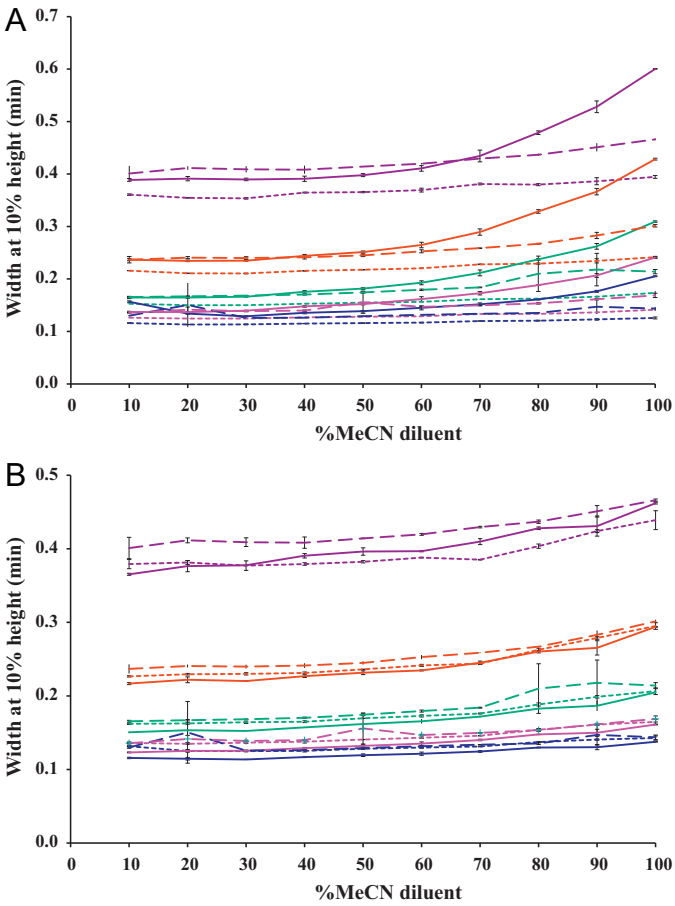

Fig. 3. Change in peak width at 10% height with injection solvent strength with (A) constant injection mass of 30 μg mass, varied volume (solid line – 30 μL, dashed line – 15 μL, and dotted line – 7.5 μL) and (B) constant 15 μL volume, varied mass (solid line – 60 μg, dashed line – 30 μg, and dotted line – 15 μg). Analytes as Fig. 2. Column: Poroshell 120 EC-C18.

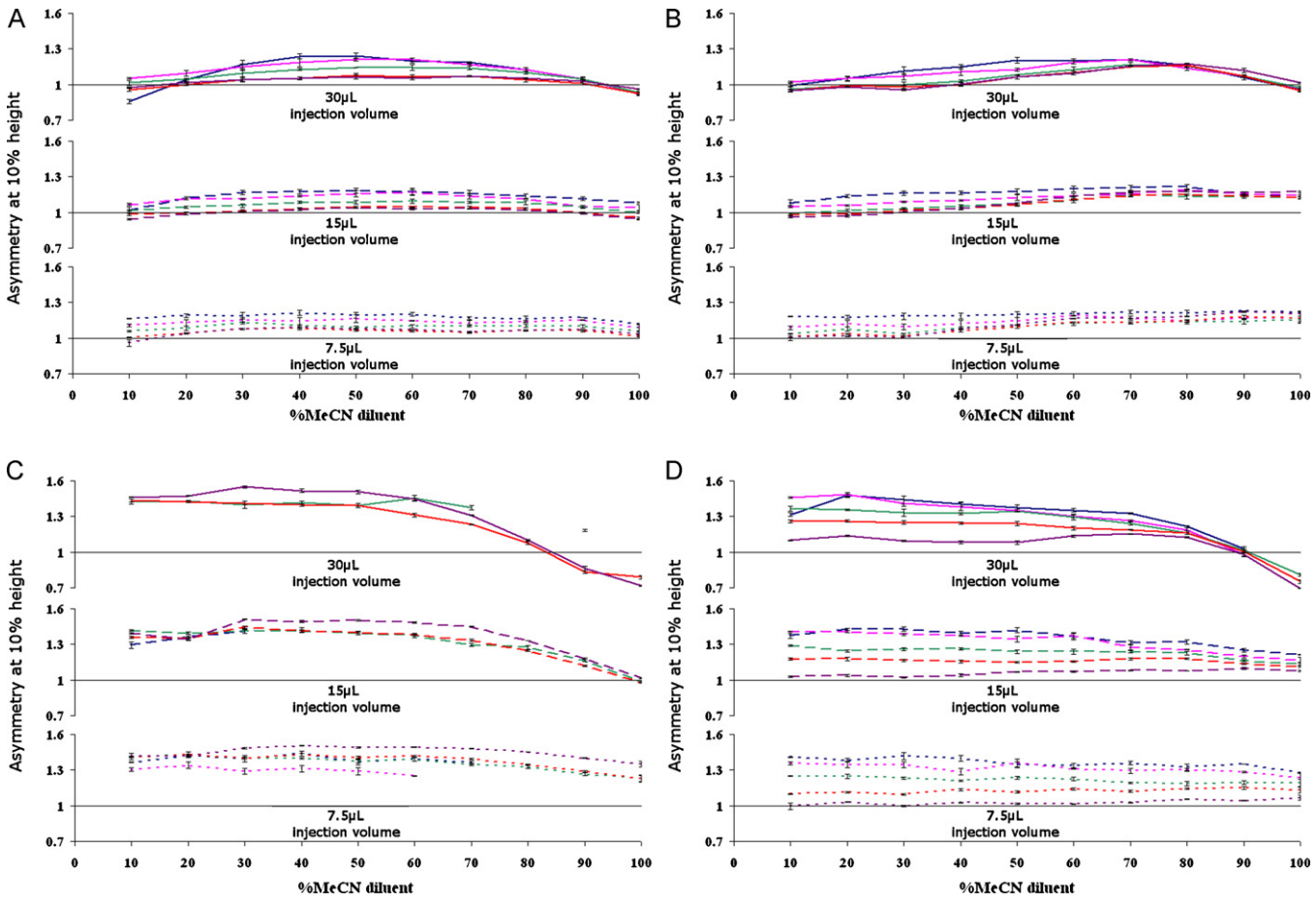

Fig. 4. Change in asymmetry at 10% height with injection solvent strength with constant 30 μg injection mass for the (A) Poroshell 120 EC-C18, (B) Zorbax Stablebond-C18, (C) Zorbax 300Extend-C18, and (D) Zorbax Bonus-RP. Analytes: acetone – dark blue, 2-butanone – pink, 2-pentanone – green, 2-hexanone – red, 2-heptanone – violet. (For interpretation of the references to color in this figure legend, the reader is referred to the web version of the article.)

injection volume reduces the increase in width with injection solvent strength. The change in width is mostly responsible for the reduction of efficiency, and therefore sensitivity to injection solvent strength. The major difference between the reductions of efficiency due to the injection solvent among the four columns tested is the magnitude of the change in width as injection solvent is strengthened. On the Poroshell column, there is a 67% efficiency decrease of 2-heptanone due solely to the increase in width from the maximum efficiency at the 1.25 μL, 5 μg, 100% MeCN injection (low volume, low mass) to the minimum efficiency of the 30 μL, 30 μg, 100% MeCN.

In Figs. 4A–D and 5A–D, the asymmetries of the analytes on the column studied are plotted as a function of the injection solvent strength, volume, and mass. The asymmetry functions are significantly different for each column. The only similarity among the columns is that the asymmetry near the mobile phase concentration (40% MeCN) is constant despite changes in volume or mass. Any changes in measured asymmetry from changing the injection volume or mass are only evident with injection solvent strengths that are stronger or weaker than the 40%MeCN mobile phase and the change is greater the further the injection solvent strength is from the mobile phase. In other words, the asymmetry of the 60%MeCN injections depend less on volume and mass than the 90%MeCN injections. Notably, when reducing the volume from 30 μL to 7.5 μL, the curve of the plot of asymmetry vs. injection solvent of the early eluting acetone is flattened to depend less on the injection solvent strength, and the later eluting 2-heptanone is mostly unaffected. However, when reducing the mass, acetone is mostly unaffected and there is a gradient of flattening as retention factor is increased. The curve of asymmetry vs. injection solvent of 2-Butanone is less dependent on mass than the curve of 2-heptanone. The relationship between asymmetry and volume holds for all four columns tested (Fig. 4A–D), however the effect of injection mass is only evident on the Poroshell (Fig. 5A) and the Stablebond phase (Fig. 5B). For the 300Extend (Fig. 5C) and Bonus-RP phase (Fig. 5D) there is no significant relationship between asymmetry and injection mass.

To quantify and compare the effect of injection solvent strength on each column, we first define the efficiency curve with the vector of efficiency, $\vec{N}$, vs. injection solvent compositions, N_i, where i is the ordered value of acetonitrile percentage.

$$\vec{N} = \langle N_1, N_2, N_3, \ldots, N_i \rangle \tag{10a}$$

For each column, injection volume, and mass, we can construct measured and ideal vectors. For this work, measured efficiency vectors are constructed as above where the i value ranges from 10% to 100% MeCN in steps of 10%. Ideal efficiency vectors consist of i components equal to the maximum efficiency measured for a given injection volume and mass.

$$\vec{N}_{\text{ideal}} = \langle N_{\max}, N_{\max}, N_{\max}, \ldots, N_i \rangle \tag{10b}$$

We may project the measured vector onto the ideal vector, then normalize the magnitudes, such that $0 < s < 1$, and represents the cumulative percentage loss of efficiency: the sensitivity, s

$$s = \frac{\vec{N}_{\text{measured}} \cdot \vec{N}_{\text{ideal}}}{\|\vec{N}_{\text{ideal}}\|^2} = \frac{\sum_{n=1}^{i} (N_{\text{measured},n}/N_{\text{ideal},n})}{i} \tag{11}$$

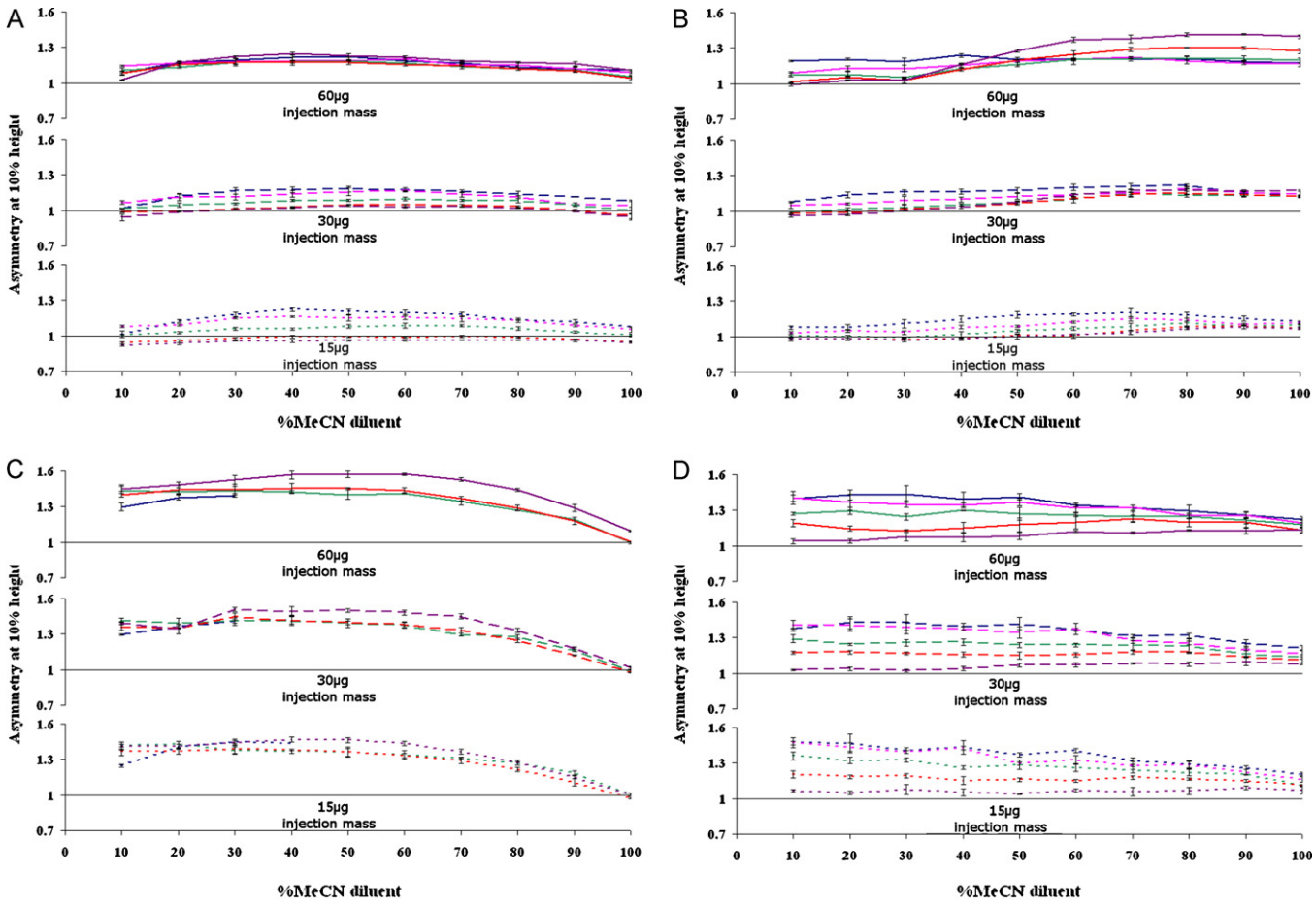

Fig. 5. As Fig. 4, but with constant 15 µL injection volume for the (A) Poroshell 120 EC-C18, (B) Zorbax Stablebond-C18, (C) Zorbax 300Extend-C18, and (D) Zorbax Bonus-RP.

By this calculation, s is independent of the maximum efficiency of the column, allowing columns of different plate counts to be directly compared. s is dependent on the percentage change of the plate count, and not the value of the change. In the ideal case, where the efficiency does not decrease with injection solvent strength, $s = 1$. If the efficiency decreases by 2% for each 10% MeCN increase in injection solvent, then $s = 0.915$. For a 5% decrease per 10% MeCN increase, $s = 0.803$. To our knowledge, it has not been suggested in the literature that particle diameter nor column length affect the injection solvent sensitivity of a column, though it is reasonable to expect a dependency on column internal diameter. If the efficiency vector cannot be modeled by a straight line, the sensitivity is then a function of the percentage step change in injection solvent, 10% MeCN in this study. In practice, the non-linear increase in width with increasing injection solvent is the dominant factor in reducing the efficiency, therefore measured sensitivity values are a function of the percentage step change in solvent strength.

Table 2 lists the sensitivity of each column at each injection volume and mass, and Fig. 6A and B plots those values as a function of injection volume and injection mass, respectively, for 2-hexanone and 2-heptanone. The Stablebond-C18 phase is the most ideal column tested, having very little sensitivity to the injection solvent, whereas the 300Extend-C18 and Bonus-RP are the most sensitive to injection solvent. There is also a dependence of retention factor on sensitivity, for example the top row of Table 2 has a greater sensitivity value for acetone and 2-hexanone than for 2-butanone or 2-pentanone. The mathematical reason is the percentage increase in width is different for each analyte. For instance, 30 µg in 30 µL injection onto the Poroshell, the width of acetone changes from 0.14 min at 20% MeCN to 0.21 min at 100% MeCN, an increase of 50%. The width of 2-pentanone over the same span increases 85% and the width of 2-heptanone increases 54%. Since width increase is the dominant factor in the decrease in the sensitivity value, the trends follow. The physicochemical reason for this retention-factor-dependent width increase is unknown.

In an attempt to explain the differences of the sensitivity, we have characterized these four columns via the different contributions to retention of the hydrophobic-subtraction model.

4.2. Comparison to the hydrophobic-subtraction model

Column and solute parameters for the four columns and analytes studied are listed in Table 3, as well as the retention factors for the methyl ketones with the H-S mobile phase. To regress the solute parameters for the methyl ketones and lidocaine, five additional columns were characterized, selected randomly from on-hand supplies, in addition to the three alkyl silica columns (non-polar embedded): Agilent Zorbax 300Stablebond-C18, AMT Halo C18, Supelco Discovery C18, Waters XterraMS C18, and YMC Pack-Pro C18. For lidocaine solute parameters, the YMC PackPro was removed from the set due to a retention factor of 0.000 ± 0.000, i.e., unretained. Deviations from published column parameters [20,32] are likely due to column aging shown by a decrease in H parameter, and an increase in A and C parameters [32]. Each column gave retention time reproducibility of <0.005 min and a reasonably small standard deviation for the regression <0.015. Compared to the literature values, each column gave a $\cos(\theta)$ between 0.97 and 1.00 for the dot product, with the least being the Bonus-RP. The deviations seen in the H-S model for polar embedded phases have been described well [21], and our data follow the general

Table 2
Measured sensitivities for all columns, conditions, and analytes. Some values not reported due to peak overlap.

	Conc. (mg/mL)	Mass (μg)	Volume (μL)	Acetone	Butanone	2-Pentanone	2-Hexanone	2-Heptanone
Poroshell EC-C18	1.0	30	30	0.752 ± 0.004	0.687 ± 0.006	0.676 ± 0.006	0.718 ± 0.006	0.793 ± 0.008
		15	15	0.894 ± 0.008	0.851 ± 0.004	0.823 ± 0.008	0.858 ± 0.007	0.910 ± 0.011
	2.0	30	15	0.893 ± 0.012	0.820 ± 0.013	0.739 ± 0.010	0.806 ± 0.009	0.871 ± 0.012
		60	15	0.875 ± 0.005	0.830 ± 0.005	0.812 ± 0.006	0.807 ± 0.006	0.771 ± 0.006
	4.0	30	7.5	0.944 ± 0.006	0.912 ± 0.004	0.906 ± 0.004	0.909 ± 0.004	0.914 ± 0.002
		5	1.25	0.983 ± 0.004	0.986 ± 0.005	0.981 ± 0.004	0.975 ± 0.005	0.968 ± 0.003
Zorbax 300Extend-C18	1.0	30	30				0.588 ± 0.006	0.593 ± 0.004
		15	15			0.750 ± 0.007	0.755 ± 0.007	0.766 ± 0.004
	2.0	30	15			0.757 ± 0.006	0.766 ± 0.005	0.700 ± 0.007
		60	15				0.729 ± 0.006	0.640 ± 0.006
	4.0	30	7.5			0.891 ± 0.007	0.869 ± 0.006	0.782 ± 0.004
		5	1.25		0.977 ± 0.007	0.980 ± 0.005	0.978 ± 0.005	0.964 ± 0.006
Zorbax Stablebond-C18	1.0	30	30	0.849 ± 0.022	0.806 ± 0.019	0.839 ± 0.016	0.828 ± 0.025	0.858 ± 0.017
		15	15	0.914 ± 0.014	0.930 ± 0.013	0.944 ± 0.010	0.930 ± 0.021	0.885 ± 0.007
	2.0	30	15	0.917 ± 0.016	0.890 ± 0.015	0.903 ± 0.012	0.957 ± 0.012	0.973 ± 0.015
		60	15	0.906 ± 0.016	0.883 ± 0.013	0.846 ± 0.011	0.852 ± 0.009	0.835 ± 0.009
	4.0	30	7.5	0.934 ± 0.017	0.963 ± 0.028	0.955 ± 0.014	0.949 ± 0.015	0.964 ± 0.011
		5	1.25	0.969 ± 0.011	0.962 ± 0.015	0.961 ± 0.007	0.962 ± 0.012	0.971 ± 0.013
Zorbax Bonus-RP	1.0	30	30			0.562 ± 0.010	0.546 ± 0.008	0.590 ± 0.019
		15	15	0.860 ± 0.029	0.811 ± 0.026	0.758 ± 0.009	0.739 ± 0.018	0.726 ± 0.012
	2.0	30	15	0.823 ± 0.011	0.826 ± 0.021	0.748 ± 0.018	0.725 ± 0.009	0.761 ± 0.030
		60	15	0.816 ± 0.017	0.808 ± 0.010	0.763 ± 0.019	0.757 ± 0.027	0.755 ± 0.012
	4.0	30	7.5	0.920 ± 0.012	0.892 ± 0.015	0.886 ± 0.009	0.879 ± 0.023	0.869 ± 0.023
		5	1.25	0.983 ± 0.016	0.970 ± 0.013	0.956 ± 0.015	0.961 ± 0.016	0.982 ± 0.015

trend that the Bonus-RP is significantly less acidic (lower A and C), more basic (higher B), and more polar (lower H) than type-B alkyl silica.

As the carbon number is increased, the solute parameters for the methyl ketones become more hydrophobic (less negative η') and less hydrogen bond acidic (less negative α'), as expected. With the remaining parameters, the trends are not as clear, and the calculated solute parameters for the acetophenone control deviate from the published literature values. The greatest standard error from the regression is found on the σ' and α' parameters, as is common for data sets with low column numbers [33]. Important to our study is the relative contribution of the hydrogen bond basicity β' is constant with increasing carbon number, and the hydrogen bond acidity α' increases with carbon number. By understanding the mechanisms of retention for these analytes, differences in the effects of the injection solvent strength regarding asymmetry can be explained. Though the solute parameters, by convention, change with separation conditions, it is not expected that the trends would be different, i.e., one would not expect the hydrophobic contribution to retention to be less for 2-heptanone than for acetone in any mobile phase. However, it can be posited that the relative contributions of each parameter to change with separation conditions, i.e., the η' may play less of a role than β' in highly aqueous phases for the retention of acetone vs. the retention of 2-heptanone. As the H-S model has developed into a method of column comparison, there have been no published comparisons of solute parameter changes

Table 3
Column and solute parameters measured by the hydrophobic-subtraction model.

	H	S*	A	B	C(2.8)	SD
Poroshell 120 C18	1.023 ± 0.005	−0.012 ± 0.007	−0.139 ± 0.014	0.021 ± 0.005	0.202 ± 0.010	0.009
Zorbax 300Extend-C18	0.993 ± 0.003	0.014 ± 0.004	−0.050 ± 0.008	0.015 ± 0.003	0.242 ± 0.006	0.005
Zorbax Stablebond-C18	1.003 ± 0.004	−0.037 ± 0.005	0.224 ± 0.010	−0.001 ± 0.004	0.214 ± 0.008	0.007
Zorbax 300Stablebond-C18	0.881 ± 0.007	−0.061 ± 0.009	0.107 ± 0.019	0.046 ± 0.007	0.283 ± 0.014	0.012
Zorbax Bonus-RP	0.730 ± 0.026	0.043 ± 0.020	−0.435 ± 0.071	0.261 ± 0.022	−1.492 ± 0.052	0.047
AMT Halo C18	1.117 ± 0.005	0.036 ± 0.007	−0.010 ± 0.014	−0.032 ± 0.005	0.052 ± 0.010	0.009
Supelco Discovery C18	0.947 ± 0.005	0.014 ± 0.007	0.046 ± 0.014	0.018 ± 0.005	0.194 ± 0.011	0.009
Waters XterraMS C18	0.987 ± 0.001	0.007 ± 0.001	−0.102 ± 0.003	−0.009 ± 0.001	0.137 ± 0.002	0.002
YMC PackPro C18	0.988 ± 0.006	−0.012 ± 0.008	−0.053 ± 0.016	0.000 ± 0.006	−0.193 ± 0.012	0.010

	η'	σ'	β'	α'	κ'	SD
Acetone	−1.452 ± 0.005	−0.009 ± 0.215	0.078 ± 0.042	−1.205 ± 0.255	0.065 ± 0.031	0.010
Butanone	−1.172 ± 0.007	−0.372 ± 0.275	0.038 ± 0.054	−1.170 ± 0.327	0.011 ± 0.039	0.013
2-Pentanone	−0.927 ± 0.001	−0.181 ± 0.031	0.042 ± 0.006	−0.649 ± 0.037	0.030 ± 0.004	0.001
2-Hexanone	−0.695 ± 0.002	−0.222 ± 0.074	0.043 ± 0.015	−0.395 ± 0.088	0.027 ± 0.011	0.003
2-Heptanone	−0.463 ± 0.003	−0.159 ± 0.106	0.081 ± 0.021	0.038 ± 0.126	0.008 ± 0.015	0.005
Lidocaine	−2.179 ± 0.094	−0.053 ± 0.803	−0.084 ± 0.170	−2.934 ± 1.875	1.897 ± 0.566	0.037
Acetophenone	−0.748 ± 0.001	−0.335 ± 0.033	0.024 ± 0.007	−0.356 ± 0.039	0.007 ± 0.005	0.002
Acetophenone (Lit)	−0.744	0.133	0.059	−0.152	−0.009	

Retention factors (k')	Acetone	Butanone	2-Pentanone	2-Hexanone	2-Heptanone
Poroshell EC-C18	0.415 ± 0.001	0.783 ± 0.002	1.477 ± 0.002	2.833 ± 0.003	5.587 ± 0.006
Zorbax SB-C18	0.558 ± 0.001	1.022 ± 0.001	1.895 ± 0.002	3.587 ± 0.003	6.919 ± 0.006
Zorbax 300Extend-C18	0.208 ± 0.001	0.357 ± 0.001	0.637 ± 0.000	1.176 ± 0.000	2.263 ± 0.001
Zorbax Bonus-RP	0.448 ± 0.004	0.813 ± 0.004	1.462 ± 0.006	2.614 ± 0.009	4.734 ± 0.015

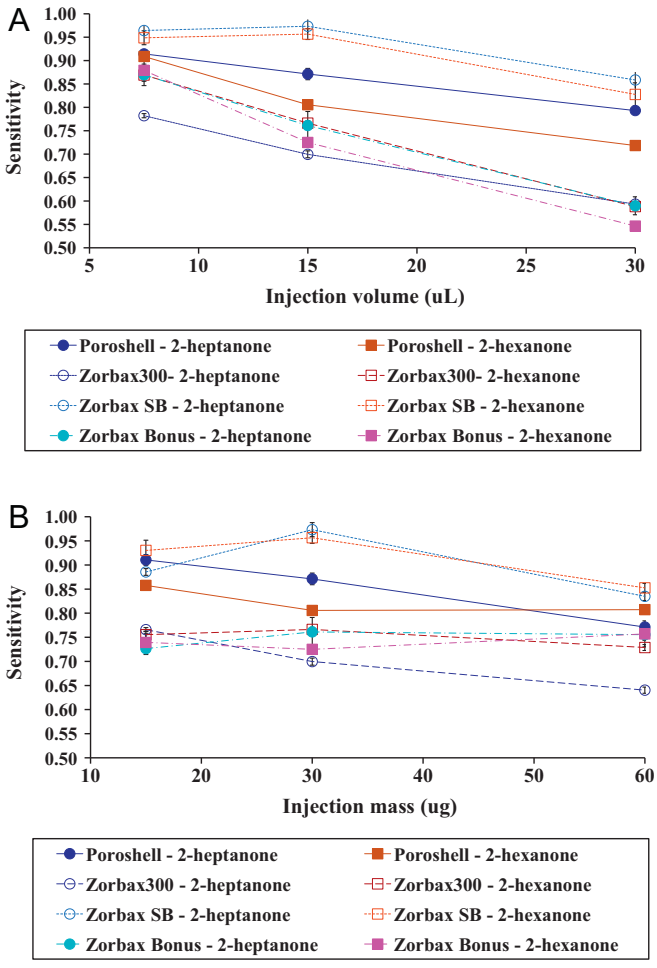

Fig. 6. Sensitivity of all columns tested as a function of (A) injection volume, with a constant 30 μg mass or (B) injection mass, with a constant 15 μL volume. Values calculated from Eq. (2) for 2-hexanone and 2-heptanone.

with separation conditions, to our knowledge, other than for the κ' value changing with pH of the mobile phase.

Two trends have been noted with the plots of asymmetry vs. injection solvent: more ideal curves for low k' analytes with a reduction of injection volume (all columns) and a gradient of ideality with k' with a reduction in injection mass (few columns). We refer to ideality here in the same manner as Section 4.1, where an ideal curve of the plot of asymmetry vs. injection solvent is not a function of the injection solvent strength. Any dependence on injection solvent strength is a deviation from ideality. If the change in ideality of asymmetry is a qualitative model of the change in retention parameters of the analytes within the injection solvent, then it suggests that the change with injection volume are more likely to elucidate any underlying physicochemical phenomena taking place as a function of thermodynamics (Fig. 4A–D), whereas the change in asymmetry with change in mass is probably a change in linearity of the isotherm caused by overloading (Fig. 5A–D).

Reductions in the asymmetry value with weaker injection solvents than the mobile phase have been reported as caused by focusing the tail of the analytes on the head of the column, and a greater reduction has been seen for low k' analytes. This trend seen as a function of the η'H contribution to retention, and is noticeably greater in Fig. 4A and B on the more hydrophobic (higher H) Poroshell and Stablebond columns, but not evident on the less hydrophobic polar embedded Bonus-RP phase, Fig. 4D. With lower injection volume, there is less time spent in the injection solvent,

Table 4
Fitting parameters for Eq. (7).

	Poroshell EC-C18	Stablebond-C18	300Extend-C18	Bonus-RP
t	3.04	2.37	4.09	2.54
ε	0.79	0.62	0.75	0.60
K(C18)	4.27	5.62	3.79	5.65
K(OH)	0.041	0.042	0.069	0.038
K(C18)/K(OH)	103.2	133.0	54.9	149.7

and therefore less focusing effect which is only evident on the least retained compounds as the time spent in the injection solvent is a function of the k'. With injection solvents that are stronger than the mobile phase, the front of the analyte band is carried by the stronger injection solvent along some length of column. The injection solvent strength at which the asymmetry significantly deviates correlates well with the silanol activity; A term in Eq. (3). The greater silanol activity of the non-endcapped Stablebond phase (Fig. 4B) allows for a greater strength of the injection solvent before significant fronting is seen on the peak when compared to the endcapped Poroshell EC (Fig. 4A) or 300Extend phases (Fig. 4C).

Furthermore, from the sensitivity values of Table 2 and the retention factors in Table 3, a general trend that the more retentive a phase the better the sensitivity value. For 2-heptanone the sensitivity vs. retention factor correlates well with respect to injection volume (7.5 μL, $r^2 = 1.000$; 15 μL, $r^2 = 0.991$; 30 μL, $r^2 = 0.998$), but for 2-hexanone the correlation is weaker (7.5 μL, $r^2 = 0.955$; 15 μL, $r^2 = 0.740$; 30 μL, $r^2 = 0.884$). The retention factors of the Bonus-RP column do not fit well with the other C-18 columns and were removed for these r^2 values. However, one cannot compare the absolute retention of a phase without discussing the chemistry of the analyte. The H-S model quantifies the contribution to retention of five different column-analyte interactions and can be used to compare the absolute retention between columns.

Consequently, we find a correlation of the sensitivity to the ratio of H/A for the column, as seen in Fig. 7A. Other correlations have significantly lower r^2 values for the fit: H/S – 0.66, H/B – 0.49, H/C – 0.64. Again, the Bonus-RP does not fit well with the C18 columns, which can be due to the precision of the column parameters in the method or can be indicative of a differing dependence of sensitivity on H-S parameters for the amide phases. The correlation of H/A and sensitivity to injection solvent strength is likely related to the ability of the column to retain both components of the hydro-organic mixture, i.e., the acetonitrile is retained strongly by a higher H value and the water is retained by a non-negative A value (non-endcapped). Further investigation in the physical meaning of this correlation was done by measuring the acetonitrile excess adsorption isotherm. Overall, this correlation suggests a quick test to predict the sensitivity of a column to injection solvent strength or volume, and given the large number of alkyl-silica columns in the USP-PQRI database, one that may prove useful to chromatographic method development.

4.3. Comparison to the acetonitrile excess adsorption isotherm

Measurement of the acetonitrile isotherm was done for the four studied columns and these are shown in Fig. 8. Positive portions of the isotherm are indicative of adsorption of acetonitrile onto the stationary phase ligand, and negative portions are due to the adsorption of water onto the residual silanols. Values from the fit of Eq. (7) are reported in Table 4. As can be seen, endcapped phases' ε values are closer to unity and therefore are more homogenous. However the correlation between heterogeneity and sensitivity is weak, $r^2 \approx 0.25$. Better correlation can be seen with number of acetonitrile monolayers (Fig. 7B, $r^2 \approx 0.98$) and the ratio of the distribution constant between the C18 ligand and acetonitrile (K_{C18})

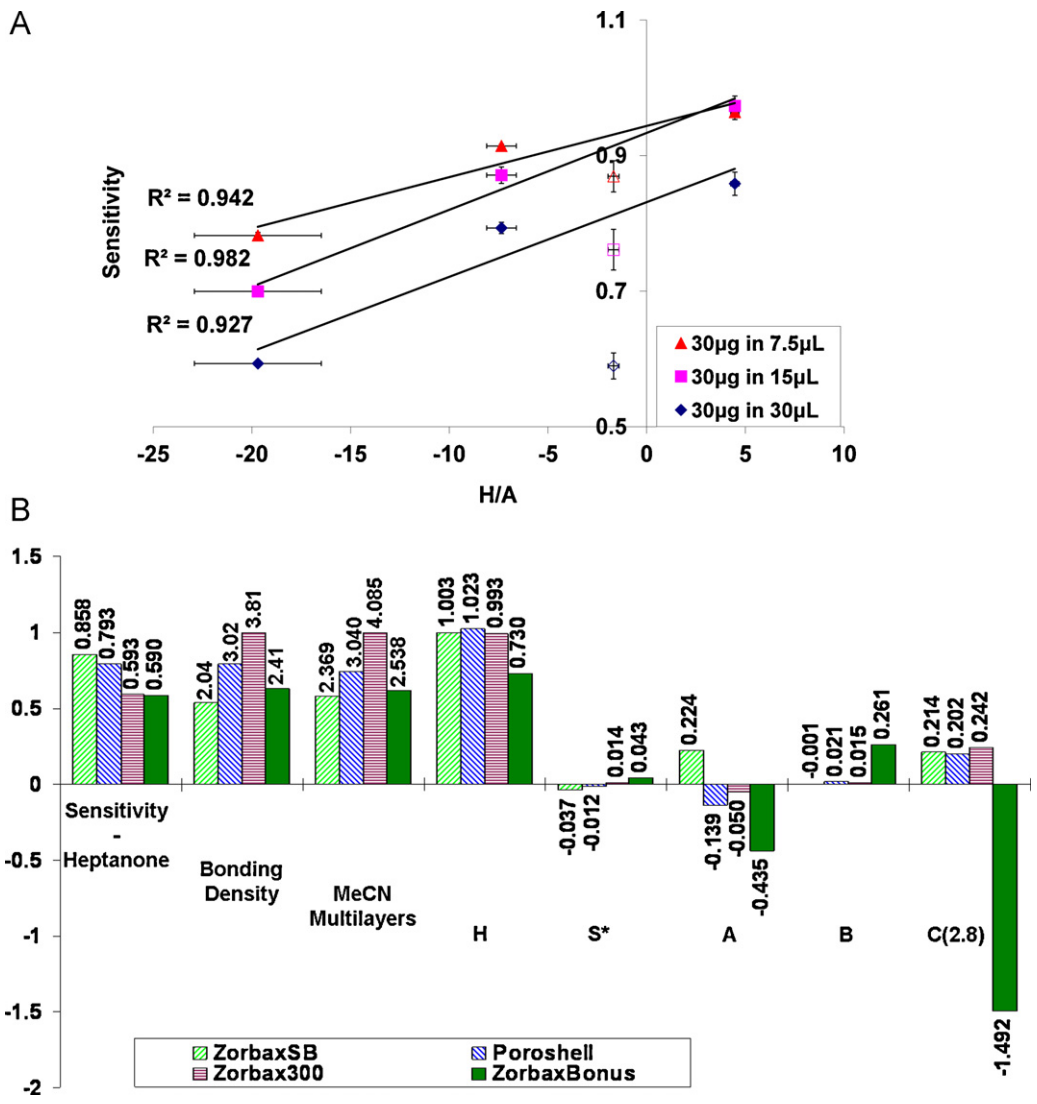

Fig. 7. Comparison of sensitivity values for 30 µg of 2-heptanone in 30 µL to (A) to ratios of column parameters, H/A. Open shapes refer to the Zorbax Bonus-RP phase, and (B) bonding density (µmol/m^2), number of sorbed acetonitrile layers, and column parameters for the hydrophobic-subtraction model.

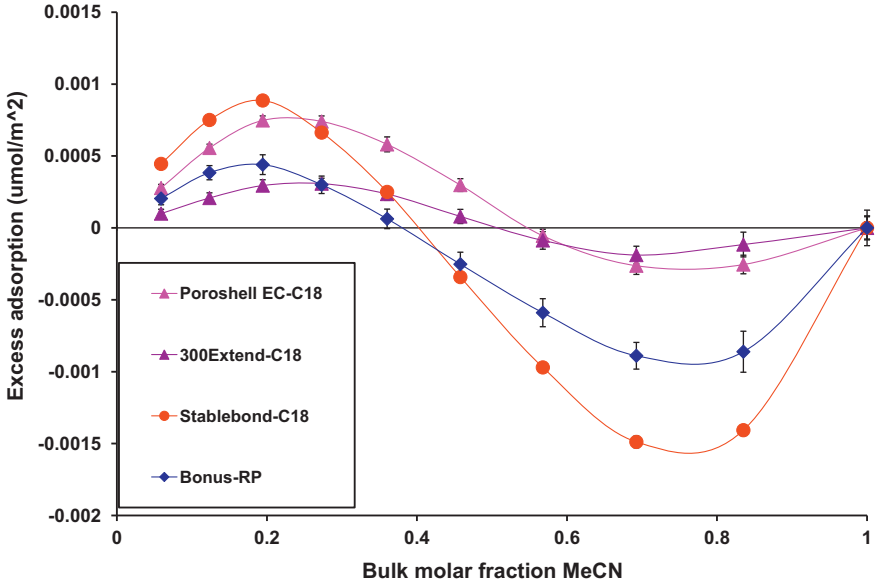

Fig. 8. Measured acetonitrile excess isotherms from Eqs. (4a) and (4b).

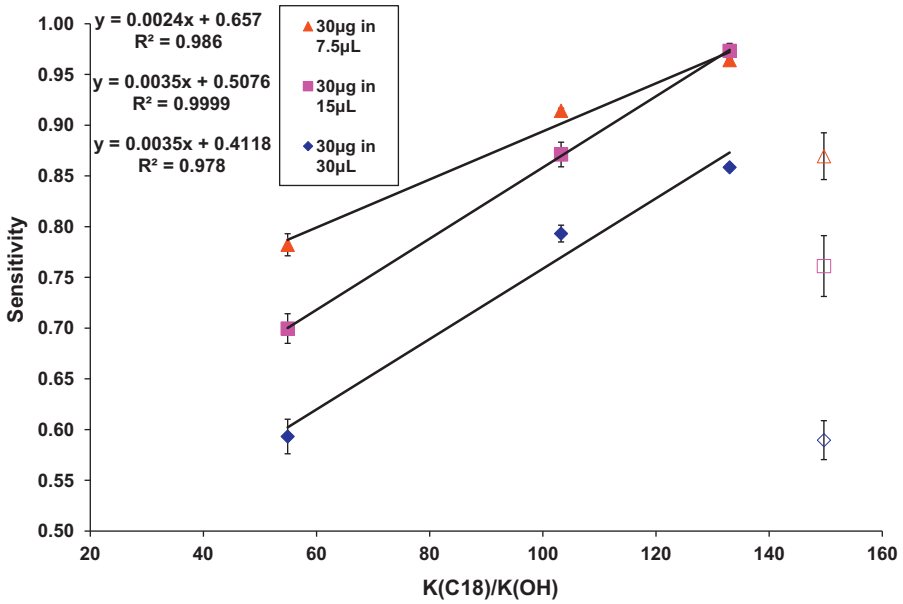

Fig. 9. Correlation between K(C18)/K(OH) and sensitivity for values of 30 μg of 2-heptanone. Closed symbols: C18 phases. Open symbols: polar embedded.

to the distribution constant between the residual silanols and acetonitrile (K_{OH}), as seen in Fig. 9. The correlation of the distribution constant ratio and sensitivity can be considered similar to the correlation seen in Section 4.2 with the ratio of H/A and sensitivity. This suggests that the sensitivity to injection solvent strength is related to the ability of the column to retain both components of the hydro-organic mixture. The greater the retention of components of the injection solvent, the less the change in band shape with changes in the injection parameters. However, in all considered correlations the Bonus-RP phase is an outlier, which further supports that there is a differing dependence for polar-embedded phases.

The strong negative correlations between sensitivity and bonding density and number of sorbed acetonitrile layers in Fig. 7B are both indicative of the same phenomena [27], and so offer no additional conclusions. However, the number of sorbed layers and the conclusions of Ref. [34] on the sensitivity to differing organic modifiers in the injection solvent in the HILIC mode can provide predictions on other modifiers not studied in this work. Ruta et al. found that the injection solvents are modeled as a step change in mobile phase solvent strength, and for HILIC solvent strength can be listed as MeCN < IPA < EtOH < MeOH < H_2O from weakest to strongest [34]. It is reasonable to expect the exact reverse for RPLC, and can be correlated with the thickness of the adsorption layer, which can be expected to increase with carbon number. From Refs. [26,27], roughly, MeOH forms a single monolayer, EtOH forms two monolayers, and IPA, THF, and MeCN form three monolayers. It is predicted then that injection solvent sensitivity values would trend as MeOH > EtOH > IPA ≈ THF ≈ MeCN.

An interesting case to predict would be a ternary system where the injection solvent is not matched by the organic modifier of the mobile phase. In 2010, Coym measured the energetic contribution to retention using a ternary mobile phase of X% MeOH:(50-X%) MeCN:50% H_2O [35]. It was found that the enthalpic contribution to retention remained constant, whereas the entropic contribution decreased with increasing MeOH concentration, as well as general trends in the coefficients of the Linear Solvation Energy Relationship model of retention. Contribution of cavity formation v, excess polarizability e, and hydrogen bond basicity a increase as MeOH is added to the mobile phase and favor retention. Polar interactions s and constant c decrease with MeOH concentration and favor elution, whereas the hydrogen bond acidity is roughly constant. Cavity formation and hydrogen bond basicity are the major factors in retention, so predictions can be made mostly upon the general trend with these two parameters. Then, the same prediction as above would hold within a ternary system where an injection-solvent modifier mismatches with the mobile phase: MeOH > EtOH > IPA ≈ THF ≈ MeCN. As can be seen by molecular simulation in Ref. [36] by Rafferty et al., protic solvents replace sorbed water at silanols, which would serve to reduce the silanol effect on injection solvent sensitivity and relatively increase the ligand effect on injection solvent. Expectedly, then, acetonitrile as an injection solvent modifier injected into an aqueous methanol mobile phase would produce a less ideal sensitivity (lower s value from Eq. (11)) than the exact juxtaposition – methanol injected into an acetonitrile mobile phase.

4.4. Injection solvent sensitivity of lidocaine

Similar to methyl ketones, lidocaine is soluble in a range of aqueous-MeCN mixtures, and with a pK_a of 7.9, any effect of a change in ionization state due to the injection solvent should be apparent. It has been shown that ionizable compounds show an increased sensitivity to injection solvents compared to non-polars [34,37]. Chromatograms of lidocaine were obtained with stepped injection solvents as in Section 4.1 with one-tenth the injection mass. As the methyl ketone data, near ideal sensitivity values (s > 0.9) are measured for the 1.25 μL injection volume on each column, and decreased ideality with increased injection volume. For the Stablebond-C18, each injection volume and strength produced an easily integrated peak that followed the general trends of the methyl ketones in that less injection strength and less injection volume produced a narrower concentration band, and thus a higher plate count. However, there was significant band splitting on the endcapped, non-polar embedded Poroshell EC-C18 and Zorbax 300Extend-C18 columns above some threshold MeCN concentration of the injection solvent. With a high organic injection solvent, the lidocaine injection band was dragged down the column producing a shoulder or a split peak. As injection volume is increased, the threshold organic concentration for the shoulder to appear was decreased, but was independent of the injection mass. Though, it

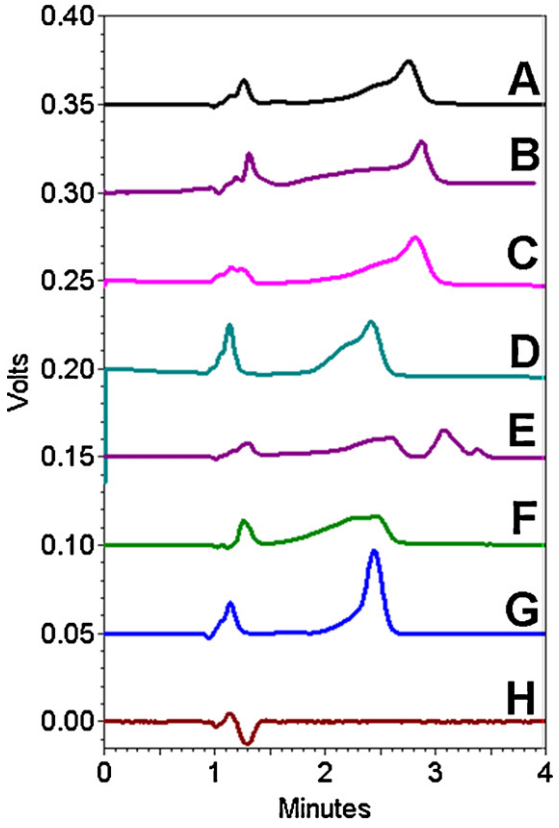

Fig. 10. Lidocaine peak shape with changes in the 15 μL of 80% MeCN injection solvent onto the Poroshell column. X and Y axes have been scaled to ease comparison. From top to bottom: A – 1.00 mL/min flow rate, 25 °C. B – 0.10 mL/min flow rate. C – 1.00 mL/min, 10 mM citrate. D – 10 mM citrate, 50 °C. E – 10 mg/mL TBA-HFP added. F – 1.0 mg/mL TBABr only. G – 10 mM citrate, 50 °C, 10 mg/mL TBA-HFP. H – Blank at 190 nm.

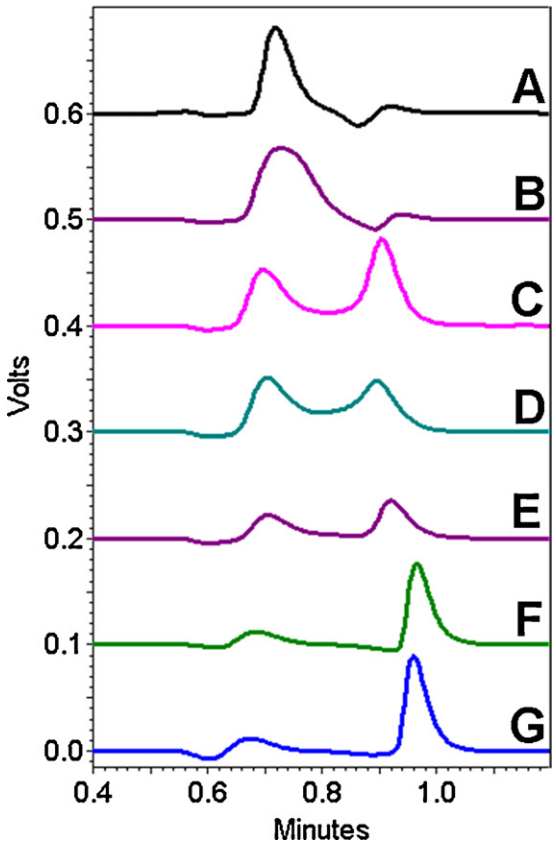

Fig. 11. Lidocaine peak shape with changes in the injection volume of 10% MeCN injection solvent onto the Bonus-RP column. Y axis has been scaled to ease comparison. From top to bottom: A – 1.25 μL of 0.4 mg/mL lidocaine. B – 7.5 μL of 0.4 mg/mL lidocaine. C – 15 μL of 0.4 mg/mL lidocaine. D – 15 μL of 0.2 mg/mL lidocaine. E – 15 μL of 0.1 mg/mL lidocaine. F – 30 μL of 0.1 mg/mL lidocaine, day 1. G – 30 μL of 0.1 mg/mL lidocaine, day 2.

can be expected that injection masses that overload the column would reduce the threshold organic concentration.

It could be considered that the peak's shoulder could be mitigated by buffering the injection solvent, the addition of an ion pairing reagent, or by changing the column temperature. To the 10%, 20%, 30%, 40%, and 80% MeCN injection solvents, citric acid and monosodium citrate was added, isotonic with respect to the mobile phase. There was no measurable change in the peak shape. 1 mM and 10 mM tetrabutyl ammonium hexafluorophosphate (TBA^+, HFP^-) was added to the buffered 80% MeCN injection solvents to produce a significantly fronting peak, which was found to be coelution of the fronting TBA^+ with the front of the lidocaine-HFP pair. No additional change in peak shape was measured. The column temperature was increased from 25 °C to 50 °C to produce less of a shoulder, but not significantly. Fig. 10 compares the results from these runs.

For the Bonus-RP column, lidocaine eluted at the void in all injection solvent strengths above 10% MeCN invariant of the injection volume. Unlike the C18 columns, as the injection volume and strength were increased, the lidocaine peak produced a shoulder on the tail, invariant with injection mass. This result does not agree with an accepted reversed-phase retention mechanism, as the retention of an analyte should decrease with increasing solvent strength. Additionally, for the 10% MeCN injection solvent, the retention is a function of the injection volume, as shown in Fig. 11. For the 1.25 and 7.5 μL injections, the lidocaine peak is predominantly at the void. For the 15 μL injections, there is a split peak at the void and at a $k' = 0.41$, invariant with injection mass. For the 30 μL injection, the lidocaine mass is predominantly at $k' = 0.41$, occurs in each of the triplicate injections, and is reproducible from day to day. We do not have an explanation for these anomalous results, as a change in column selectivity with injection volume is not present in theory or the experimental literature.

5. Conclusions

By stepping the injection solvent strength, injection mass, and injection volume, we have measured the sensitivity of the eluting band shape to the injection solvent on four differing columns. Peak distortion occurs with increasing injection volume and solvent strength. However, with a sufficiently small injection volume (1.25 μL for 4.6 mm i.d. columns) the resulting peak is mostly invariant with injection solvent strength. For methods that require larger injection volumes, the only recourse to sharpen peak shape is to weaken the injection solvent. In the case of the Poroshell EC-C18 and Zorbax Stablebond-C18 columns, the injection mass affects the change in asymmetry with respect to injection solvent strength as a function of retention factor, with the longer retained 2-heptanone being affected to a greater extent than acetone.

Sensitivity of the C18 ligands to injection solvent effects was found to correlate with calculated bonding density, hydrophobic-subtraction model coefficients, thickness of the MeCN adsorbed layer, and the ratio of the distribution constants for the binary mobile phase sorbing to the stationary phase ligand or silanols. These correlations support a conclusion that decreased ligand activity (H or K_{C18}) and increased silanol activity (A or K_{OH}) provide a consistent peak shape with changes in injection volume or

solvent strength. The sensitivity of the polar embedded phase does not correlate with any measured value, and showed anomalous behavior with the retention of lidocaine as a function of injection volume and solvent strength.

Acknowledgements

The authors would like to thank Agilent for the donations of the Poroshell and Zorbax columns. This work was supported through a National Science Foundation grant, CHE-0717701.

References

[1] L.R. Snyder, J.J. Kirkland, J.L. Glajch, Practical HPLC Method Development, John Wiley & Sons, 1997.
[2] U.D. Neue, D.H. Marchand, L.R. Snyder, J. Chromatogr. A 1111 (2006) 32.
[3] N.E. Hoffman, S.L. Pan, A.M. Rustum, J. Chromatogr. 465 (1989) 189.
[4] N.E. Hoffman, A. Rahman, J. Chromatogr. 473 (1989) 260.
[5] M. Tsimidou, R. Macrae, J. Chromatogr. 285 (1984) 178.
[6] P.W. Wrezel, I. Chion, R. Pakula, LC–GC N. Am. 23 (2005) 682.
[7] S.A. Cohen, M.R. Schure, Multidimensional Liquid Chromatography: Theory and Applications in Industrial Chemistry and the Life Sciences, Wiley-Interscience, 2008.
[8] E. Loeser, S. Babiak, P. Drumm, J. Chromatogr. A 1216 (2009) 3409.
[9] E. Loeser, P. Drumm, J. Sep. Sci. 29 (2006) 2847.
[10] Y.V. Kazakevich, R. LoBrutto, F. Chan, T. Patel, J. Chromatogr. A 913 (2001) 75.
[11] D.V. McCalley, J. Chromatogr. A 1217 (2010) 858.
[12] P. Agrafiotou, C. Ràfols, C. Castells, E. Bosch, M. Rosés, J. Chromatogr. A 1218 (2011) 4995.
[13] J.P. Foley, J.G. Dorsey, Anal. Chem. 55 (1983) 730.
[14] C.B. Castells, R.C. Castells, J. Chromatogr. A 805 (1998) 55.
[15] R.C. Castells, C.B. Castells, M.A. Castillo, J. Chromatogr. A 775 (1997) 73.
[16] H.J. Catchpoole, R.A. Shalliker, G.R. Dennis, G. Guiochon, J. Chromatogr. A 1117 (2006) 137.
[17] R.A. Shalliker, G. Guiochon, J. Chromatogr. A 1216 (2009) 787.
[18] J.W. Thompson, T.J. Kaiser, J.W. Jorgenson, J. Chromatogr. A 1134 (2006) 201.
[19] N.S. Wilson, M.D. Nelson, J.W. Dolan, L.R. Snyder, R.G. Wolcott, P.W. Carr, J. Chromatogr. A 961 (2002) 171.
[20] L.R. Snyder, J.W. Dolan, P.W. Carr, J. Chromatogr. A 1060 (2004) 77.
[21] N.S. Wilson, J. Gilroy, J.W. Dolan, L.R. Snyder, J. Chromatogr. A 1026 (2004) 91.
[22] N.S. Wilson, M.D. Nelson, J.W. Dolan, L.R. Snyder, P.W. Carr, J. Chromatogr. A 961 (2002) 195.
[23] N.S. Wilson, J.W. Dolan, L.R. Snyder, P.W. Carr, L.C. Sander, J. Chromatogr. A 961 (2002) 217.
[24] Y.V. Kazakevich, H.M. McNair, J. Chromatogr. Sci. 33 (1995) 321.
[25] Y.V. Kazakevich, H.M. McNair, J. Chromatogr. Sci. 31 (1993) 317.
[26] F. Gritti, G. Guiochon, J. Chromatogr. A 1155 (2007) 85.
[27] F. Gritti, Y.V. Kazakevich, G. Guiochon, J. Chromatogr. A 1169 (2007) 111.
[28] B. Buszewski, S. Bocian, R. Zera, Adsorpt: J. Int. Adsorpt. Soc. 16 (2010) 437.
[29] K.B. Sentell, J.G. Dorsey, J. Liq. Chromatogr. 11 (1988) 1875.
[30] U.D. Neue, HPLC Columns: Theory, Technology, and Practice, Wiley-VCH, New York, 1997.
[31] L.R. Snyder, A. Maule, A. Heebsh, R. Cuellar, S. Paulson, J. Carrano, L. Wrisley, C.C. Chan, N. Pearson, J.W. Dolan, J.J. Gilroy, J. Chromatogr. A 1057 (2004) 49.
[32] D.H. Marchand, L.R. Snyder, J.W. Dolan, J. Chromatogr. A 1191 (2008) 2.
[33] Personal communication with Dr. Lloyd Snyder.
[34] J. Ruta, S. Rudaz, D.V. McCalley, J.L. Veuthey, D. Guillarme, J. Chromatogr. A 1217 (2010) 8230.
[35] J.W. Coym, J. Chromatogr. A 1217 (2010) 5957.
[36] J.L. Rafferty, J.I. Siepmann, M.R. Schure, J. Chromatogr. A 1218 (2011) 2203.
[37] J. Layne, T. Farcas, I. Rustamov, F. Ahmed, J. Chromatogr. A 913 (2001) 233.